Am J Physiol Lung Cell Mol Physiol 317: L57–L70, 2019.
First published March 25, 2019; doi:10.1152/ajplung.00365.2018.

RESEARCH ARTICLE

Myristoylated rhinovirus VP4 protein activates TLR2-dependent proinflammatory gene expression

J. Kelley Bentley,[1] Mingyuan Han,[1] Suraj Jaipalli,[1] Joanna L. Hinde,[1] Jing Lei,[1] Tomoko Ishikawa,[1] Adam M. Goldsmith,[1] Charu Rajput,[1] and Marc B. Hershenson[1,2]

[1]*Departments of Pediatrics and Communicable Diseases, University of Michigan, Ann Arbor, Michigan; and* [2]*Department of Molecular and Integrative Physiology, University of Michigan, Ann Arbor, Michigan*

Submitted 9 August 2018; accepted in final form 21 March 2019

Bentley JK, Han M, Jaipalli S, Hinde JL, Lei J, Ishikawa T, Goldsmith AM, Rajput C, Hershenson MB. Myristoylated rhinovirus VP4 protein activates TLR2-dependent proinflammatory gene expression. *Am J Physiol Lung Cell Mol Physiol* 317: L57–L70, 2019. First published March 25, 2019; doi:10.1152/ajplung.00365.2018.—Asthma exacerbations are often caused by rhinovirus (RV). We and others have shown that Toll-like receptor 2 (TLR2), a membrane surface receptor that recognizes bacterial lipopeptides and lipoteichoic acid, is required and sufficient for RV-induced proinflammatory responses in vitro and in vivo. We hypothesized that viral protein-4 (VP4), an internal capsid protein that is myristoylated upon viral replication and externalized upon viral binding, is a ligand for TLR2. Recombinant VP4 and myristoylated VP4 (MyrVP4) were purified by Ni-affinity chromatography. MyrVP4 was also purified from RV-A1B-infected HeLa cells by urea solubilization and anti-VP4 affinity chromatography. Finally, synthetic MyrVP4 was produced by chemical peptide synthesis. MyrVP4-TLR2 interactions were assessed by confocal fluorescence microscopy, fluorescence resonance energy transfer (FRET), and monitoring VP4-induced cytokine mRNA expression in the presence of anti-TLR2 and anti-VP4. MyrVP4 and TLR2 colocalized in TLR2-expressing HEK-293 cells, mouse bone marrow-derived macrophages, human bronchoalveolar macrophages, and human airway epithelial cells. Colocalization was absent in TLR2-null HEK-293 cells and blocked by anti-TLR2 and anti-VP4. Cy3-labeled MyrVP4 and Cy5-labeled anti-TLR2 showed an average fractional FRET efficiency of 0.24 ± 0.05, and Cy5-labeled anti-TLR2 increased and unlabeled MyrVP4 decreased FRET efficiency. MyrVP4-induced chemokine mRNA expression was higher than that elicited by VP4 alone and was attenuated by anti-TLR2 and anti-VP4. Cytokine expression was similarly increased by MyrVP4 purified from RV-infected HeLa cells and synthetic MyrVP4. We conclude that, during RV infection, MyrVP4 and TLR2 interact to generate a proinflammatory response.

asthma; cytokine; macrophage; rhinovirus; Toll-like receptor

INTRODUCTION

Rhinivirus (RV) is the most common cause of asthma exacerbations in children and adults. However, the precise mechanisms by which RV induces exacerbation are not completely known. It is well established that major group RV serotypes utilize ICAM-1 as a receptor (15) and that minor subgroup serotypes use low-density lipoprotein family receptors (18). A third group of RVs, RV-C, bind to cadherin-related family member 3 (3). Pattern-recognition receptors, including members of the Toll-like receptor (TLR) family, also play a role in sensing RV infection. We have shown that inhibition of TLR3, an endosomal receptor that interacts with double-stranded RNA, decreases RV-induced interferon expression in cultured airway epithelial cells (61). $TLR3^{-/-}$ mice infected with RV-A1B show reduced lung inflammatory responses and airway responsiveness (60).

TLR2 is a membrane surface receptor that recognizes microbe membrane constituents, such as lipopeptides and lipoteichoic acids, at the cell surface and in endosomes (42, 51). TLR2 is required and sufficient for RV-induced NF-κB activation in cultured airway epithelial and human embryonic kidney (HEK) cells (53). We subsequently showed that RV-induced cytokine expression and viral attachment are abolished in bone marrow-derived macrophages from $TLR2^{-/-}$, but not $TLR3^{-/-}$, mice (47), confirming an unexpected role for TLR2 in the RV response. Recently, we found that TLR2 was required for RV-induced airway inflammation and hyperresponsiveness in allergen-sensitized and -challenged mice and that TLR2-positive macrophages are sufficient for the response (17). RV interacts with airway macrophages after experimental infection in humans (2), and, following infection, macrophages produce chemokines essential for neutrophilic and lymphocytic inflammation (24, 28, 39, 47, 63). Together, these data suggest that TLR2 is activated during the process of RV binding and endocytosis, perhaps interacting with some component of the viral capsid.

The icosahedral RV capsid is composed of four structural subunits, viral proteins (VP) 1–4. VP1, VP2, and VP3 are arranged in a repeating symmetrical fashion on the outside of the capsid. VP4 is a small (7.5 kDa), linear, hydrophobic peptide that resides on each triangular facet of the capsid interior. VP4 and its precursor VP0 are myristoylated at the NH_2 terminus upon virus assembly (8, 10). Receptor binding induces conformational changes in the virus, including translocation of VP4 and the NH_2-terminal region of VP1 to the exterior viral surface (31). VP1 tethers the particle to the membrane, while myristoylated (Myr) VP4 (MyrVP4) forms a multimeric membrane pore, allowing extrusion of viral RNA genome into the cytoplasm (43).

Since VP4 is the only lipid-modified protein in the RV capsid, we hypothesize that VP4 serves as a ligand for TLR2. To test this hypothesis, we examined interactions of recombinant

Address for reprint requests and other correspondence: M. B. Hershenson, University of Michigan Medical School, 1150 W. Medical Center Dr., Bldg. MSRB2, Rm. 3570B, Ann Arbor, MI 48109-5688 (e-mail: mhershen@umich.edu).

VP4 and MyrVP4 with TLR2 by confocal fluorescence microscopy and fluorescence resonance energy transfer (FRET), as well as by monitoring RV- and VP4-induced cytokine mRNA expression in the presence of anti-TLR2 and anti-VP4 antibodies.

MATERIALS AND METHODS

Ethics statement. All research on human materials was approved by the University of Michigan Medical School Institutional Review Board (protocol no. HUM00042069). Parents provided written informed consent on the children's behalf. Also, children provided written assent to the research.

All animal research was performed according to the *Guide for the Care and Use of Laboratory Animals* (8th ed., National Academies Press, 2011) and the American Veterinary Medical Association *Guidelines for the Euthanasia of Animals*. The protocols were approved by the University of Michigan Animal Care and Use Committee (protocol no. PRO00006118). All mouse treatments were administered under isoflurane anesthesia. Experimental animals were humanely euthanized at defined end points by exposure to isoflurane vapors followed by thoracotomy.

Production of a peptide-directed antibody to VP4 and anti-VP4 affinity resin. We used the Jameson-Wolf antigenicity profile and DNAStar-LaserGene software to identify an antigenic 16-amino acid sequence in RV-A1B VP4 (antigen residues in boldface, Fig. 1*A*). RV-A1B VP4 protein is a hydrophobic peptide with increasing polar sequence and antigenicity toward its COOH terminus. A rabbit polyclonal peptide-specific polyclonal antiserum was generated against the 16-amino acid sequence and purified using affinity chromatography (GenScript, Piscataway, NJ). The affinity-purified antibody was added to cyanogen bromide-derivatized Sepharose (Sigma-Aldrich, St. Louis, MO) at 350 μg/mg of dry resin in 0.1 M $NaHCO_3$ (pH 8.0), washed in 0.1 M Tris·HCl (pH 7.2), and used as an affinity step for the purification of MyrVP4 from RV-infected HeLa cells (see below).

Preparation of MyrVP4 proteins. For various experiments described below, we employed three forms of MyrVP4. *1*) We used a bacterial expression system and Ni-affinity chromatography to generate and purify recombinant MyrVP4. *2*) We used urea solubilization and anti-VP4 affinity chromatography to purify MyrVP4 from RV-A1B-infected HeLa cells. *3*) We purchased synthetic MyrVP4, which was produced by chemical peptide synthesis (GenScript).

Cloning and isolation of a myristoylated recombinant VP4 protein. The cDNA sequence encoding the RV-A1B VP4 was obtained from the National Center for Biotechnology Information GenBank (accession no. D00239.1). Open reading frame cDNA was synthesized (GenScript) with a COOH-terminal 6×His tail and subcloned in-frame into pET28b (EMD Millipore, Danvers, MA) to produce pVP4. To induce myristoylation in a bacterial vector system, the open reading frame cDNA for human *N*-myristoyl transferase 1 (NMT-1; National Center for Biotechnology Information GenBank accession no. NM_021079.4) was synthesized (GenScript) and subcloned into pET11a (EMD Millipore) to produce pNMT-1. The *Escherichia coli* bacterial strain BL21(DE3) pLysS (Thermo Fisher, Waltham, MA) was transformed with pVP4 in the presence or absence of pNMT-1 and 0.5 mM myristic acid. Expression of VP4 and MyrVP4 was induced by 1 mM isopropyl thiogalactoside. Bacteria were allowed to grow for another 3 h, after which 1 mM phenylmethylsulfonyl fluoride was added and cells were centrifuged at 10,000 *g* for 30 min at 4°C and then resuspended at 20% (wt/vol) in a homogenization buffer of 8 M urea, 20 mM Tris, and 20 mM imidazole (pH 8.5) with protease inhibitor cocktail (Roche Life Science, Indianapolis, IN). A 10,000-*g* soluble fraction was obtained, batch-adsorbed to Ni-nitrilotriacetic acid agarose (Qiagen, Germantown, MD), and eluted with 100 mM imidazole base. Both the silver stain and anti-VP4 immunoblot detected a single ~10 kDa band (Fig. 1*B*). To precipitate VP4, an equal volume of 1.0 M ammonium formate (pH 6.5) was added to the eluent. After three sequential washes in deionized water to remove urea and salt, the precipitate was resuspended in DMSO and found to be endotoxin-free (*Limulus* amebocyte assay, R&D Systems, Minneapolis, MN).

Production of MyrVP4 from RV-A1B-infected HeLa cells (RV-VP4). HeLa H1 cells were grown to 90% confluence and infected with ~10^8 copies of RV-A1B in 10 ml of serum-free medium at 33°C. After 1 h, the medium was changed to 3% serum. At 48 h, plates were frozen, and HEPES (pH 7.5), NP-40, and urea were added to final concentrations of 20 mM, 0.01%, and 8 M, respectively. After addition of complete protease inhibitors (Roche Life Science), the urea was dissolved completely on a rotator at room temperature. The entire suspension was frozen, thawed, and ultrasonically disrupted for 10 min at 4°C. Particles were removed by centrifugation at 10,000 *g* for 30 min at 4°C. The soluble fraction was diluted into 10 volumes of 1 M ammonium formate (pH 6.5) and incubated at 4°C for 12 h. The resulting suspension was centrifuged at 10,000 *g* for 30 min at 4°C. The insoluble material was collected and washed sequentially with 10 mM ammonium formate and deionized water. Precipitates were resuspended in DMSO, and DMSO-insoluble particles were removed by centrifugation at 10,000 *g* for 30 min at 21°C. The DMSO-soluble fraction was diluted 1:1 with 20 mM Tris·HCl (pH 7.2) and added to anti-VP4 resin, which was mixed with the protein fraction for 1 h at 21°C. The unbound effluent was discarded, and the resin was washed with three column volumes of 50% DMSO in 10 mM Tris (pH 7.2). RV-MyrVP4 was eluted with 50% DMSO in 0.3 M glycine-acetic acid (pH 3.0), collected dropwise, neutralized with Tris to pH 7.0, and precipitated with 1 M ammonium formate, as described above. RV-MyrVP4 was suspended in DMSO for analytic and functional studies. The MyrVP4 peptide, regardless of source, was found to enter SDS-PAGE with less aggregation if diluted with a solution of 8 M urea and 1% SDS in 100 mM Tris (pH 6.5).

Production of synthetic MyrVP4. To obtain a preparation of MyrVP4 free of bacterial products, the NH_2-terminal-myristoylated 71-amino acid VP4 was produced by chemical peptide synthesis (GenScript) and dissolved in DMSO. The resulting compound was tested by GC-MS. The synthetic MyrVP4 was assessed to be 92.5% pure by GC-MS (not shown).

Fig. 1. Purification and characterization of recombinant, synthetic, and rhinovirus (RV)-derived myristoylated (Myr) virus protein-4 (VP4). *A*: amino acid sequence for RV-A1B VP4 with COOH-terminal His tag. Amino acids used for generation of a polyclonal antiserum are shown in boldface. *B*: VP4 expressed in *Escherichia coli* bacterial strain BL21(DE3) pLysS in the presence of pNMT-1 and 0.5 mM myristic acid to produce a *N*-myristoylated COOH-terminal 6×His-tagged protein. Samples were resolved by SDS-PAGE and processed for silver (*left*) or anti-VP4 (*right*) staining. Sedimented bacteria were solubilized in 8 M urea, 20 mM Tris·HCl, and 20 mM imidazole (*lane 1*). A soluble fraction was obtained by centrifugation at 10,000 *g* for 30 min (*lane 2*). The extract was batch-adsorbed to Ni-nitrilotriacetic acid-agarose (Qiagen). The column effluent is shown in *lane 3*. The column was washed with 8 M urea, 20 mM Tris·HCl, and 20 mM imidazole (*lane 4*). The column was sequentially eluted with 30 mM (*lane 5*), 40 mM (*lane 6*), or 100 mM (*lane 7*) imidazole base. Silver stain and anti-VP4 immunoblot show a ~10 kDa band (arrow). *C*: LC analysis of VP4 and MyrVP4 shows different retention times. *D*: when VP4 and MyrVP4 were processed for LC-MS, masses of 8,474.1- and 8,684.3 Da, respectively, were found, the mass difference (210 Da) being that of a single myristoyl group. *E*: HPLC analyses of synthetic MyrVP4 (GenScript) and MyrVP4 isolated and purified from RV-infected HeLa cells. *F*: to determine the myristoylated residue, the 15 most abundant ions after trypsinization and reductive alkylation were selected for MS/MS. Only the NH_2-terminal GAQVSR sequence was shifted by the size of a single myristoylation (210 Da). *G*: samples of MyrVP4 were resolved by SDS-PAGE and processed for silver (*left*) or anti-VP4 (*right*) staining. Rec, recombinant; Syn, synthetic.

Analysis of VP4 by LC-MS. Further analytic purification of a VP4 sample prepared in the presence of pNTM-1 and 0.5 mM myristic acid was achieved in formic acid and an acetonitrile gradient (0–99% over 9 min) with a C4 liquid chromatography column (Waters Xbridge BEH300, 3.5 μm) interfaced to a Thermo Fisher Q Exactive mass spectrometer (Proteomics and Peptide Synthesis Core, University of Michigan). Two peaks, a minor peak with an ion mass of 8,474.1 and a major peak with an ion mass of 8,684.3, eluted separately in time

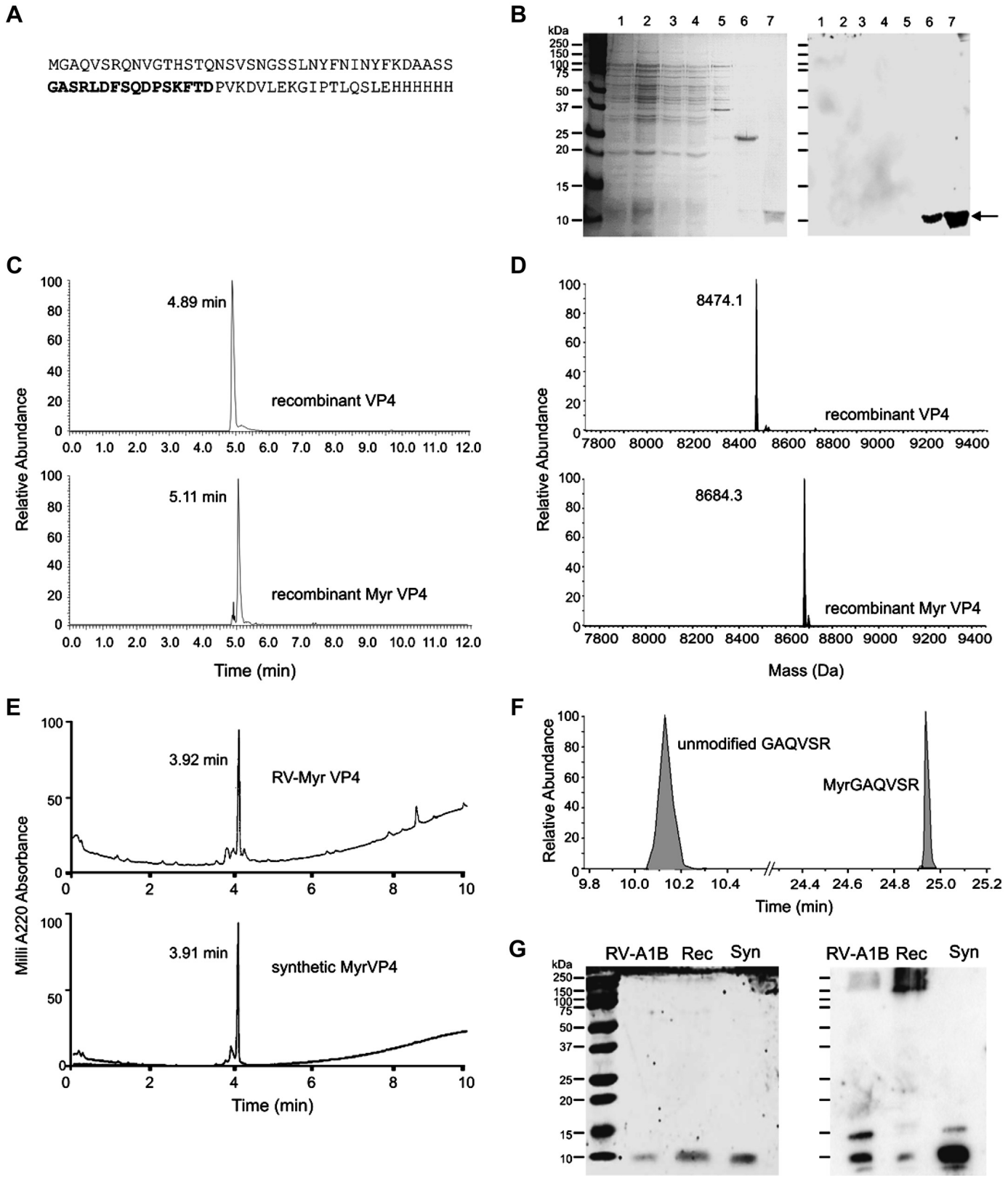

(Fig. 1*D*). The mass difference (210 Da) was that of a single myristoyl group.

Further analyses of synthetic and native RV-MyrVP4 were conducted using an Agilent 1290 analytic LC system (Santa Clara, CA) equipped with a C18 reversed-phase column with a 0.1% trifluoroacetic acid-in-water mobile phase and a 0–99% acetonitrile gradient over 9 min. On HPLC analysis, both synthetic and RV-MyrVP4 produced single major peaks eluting at 43% acetonitrile in 0.1% trifluoroacetic acid (Fig. 1*E*), indicating near 100% purity.

The myristoylation site on the recombinant MyrVP4 protein was identified and localized using SDS-PAGE, in-gel digestion with trypsin, and LC-MS/MS. Material (2 μg) was resolved by SDS-PAGE. The 8-10 kDa region was excised, digested with trypsin (Promega, Madison, WI), reduced with dithiothreitol, and alkylated with iodoacetamide. Half of the digested sample was analyzed by Nano LC-MS/MS with a Waters NanoAcquity HPLC system interfaced to a Thermo Fisher Q Exactive mass spectrometer. The 15 most abundant ions were selected for MS/MS. The remaining half of the gel digest was analyzed by a Nano LC-MS/MS-Waters NanoAcquity HPLC system interfaced to a Thermo Fisher Q Exactive mass spectrometer and a Thermo Fisher Orbitrap Velos Pro. MS/MS spectra were used to derive extracted ion chromatogram spectra of the tryptic GAQVSR sequence from the nonmyristoylated VP4 or the MyrVP4 sample. The only peptide shifted by the size of a single myristoylation (210 Da) is the NH_2-terminal GAQVSR sequence (Fig. 1*F*). In addition to MyrVP4 and VP4, the specimen contained trace amounts of murein lipoprotein (also called Braun's lipoprotein, or Lpp), a peptidoglycan-conjugated lipoprotein of the *E. coli* outer membrane.

Finally, we resolved all three MyrVP4 preparations by 15% SDS-PAGE. Each preparation showed a single silver-stained band migrating at the dye front (Fig. 1*G*). In addition, each band reacted with anti-VP4 on Western blot analysis.

Partial purification of Lpp. To test whether cellular responses to recombinant VP4 were due to contamination by the murein lipoprotein Lpp, Lpp was partially purified using a modification of the method of Braun and Rehn (4). A culture of BL21(DE3) pLysS was grown to exponential phase, centrifuged at 10,000 *g* for 5 min, resuspended in deionized water, and added to boiling 4% SDS. The suspension was mixed with heat for 4 h, cooled, and centrifuged at 10,000 *g* for 2.5 h. The sedimented pellet was washed, resuspended in TE buffer [10 mM Tris (pH 8 1) and 1 mM EDTA], and incubated with 2% (wt/vol) lysozyme for 2 h at 37°C. The digestion was stopped by addition of boiling 10% SDS to a final concentration of 1%. Insoluble material was removed by centrifugation at 10,000 *g* for 2.5 h. To precipitate Lpp, an equal volume of 1.0 M ammonium formate (pH 6.5) was added. The pellet was washed three times in 0.5 M formate buffer, lyophilized to dry, and, finally, resuspended in deionized water.

Cell culture. HEK-293 cells expressing hemagglutinin-epitope-tagged human TLR2 (293/hTLR2 cells) and the parent HEK-293 cell line that does not express TLR2 (293/null cells) were obtained from InvivoGen (San Diego, CA) and cultured in Dulbecco's minimal essential medium (Life Technologies). Cells were cultured at 1×10^5 cells/well on poly-D-lysine-coated plates. L929 supernatants were used as a source of macrophage colony-stimulating factor for isolation and culture of mouse bone marrow from C57BL/6 and $TLR2^{-/-}$ mice, as described elsewhere (47, 62). Mouse bronchoalveolar macrophages were obtained from C57BL/6 or $TLR2^{-/-}$ mice (Jackson Laboratories, Bar Harbor, ME). Mice were sensitized and challenged to ovalbumin to increase the yield of macrophages, as described elsewhere (17). Human bronchoalveolar macrophages were obtained from three asthmatic adolescents who were undergoing flexible bronchoscopy for clinical evaluation (Table 1). Mouse and human alveolar macrophages were purified by plastic adherence (38) and cultured in RPMI (Invitrogen, Carlsbad, CA) with 10% serum and 50 ng/ml human macrophage colony-stimulating factor (Peprotech) until harvested. Our previous work showed adherent cells to consist of >90% macrophages, with the rest of the cells being neutrophils. BEAS-2B human bronchial epithelial cells were grown on collagen-coated plates in bronchial epithelial growth medium (Lonza, Conshohocken, PA) containing supplements, as described elsewhere (49). Primary human airway epithelial cells were isolated from tracheobronchial trimmings of unused healthy donor lungs under a protocol approved by the University of Michigan Investigational Review Board. Cells were cultured and mucociliary-differentiated on Transwell membranes (Corning, Lowell, MA) at air-liquid interface, as described previously (48). Briefly, airway epithelial cells were cultured under submerged conditions in complete PneumaCult-Ex Plus medium (StemCell Technologies, Vancouver, BC, Canada) for 1 wk. Cells were transferred to Transwell membranes and cultured with complete medium in both the basal and apical wells until confluence was reached. Cells were maintained at air-liquid interface for 3 wk in PneumaCult air-liquid interface maintenance medium.

RV infection of cultured cells. RV-A1B was cultured in HeLa-H1 cells and partially purified by ultrafiltration, as described elsewhere (40). For determination of colocalization of VP4 and TLR2, 293/hTLR2 cells, 293/null cells, mouse bone marrow-derived macrophages, human alveolar macrophages, BEAS-2B cells, and primary human tracheobronchial epithelial cells were infected with sham or RV-A1B at multiplicity of infection (MOI) of 5 for 5 min on ice. For determination of cytokine responses, cells were infected with sham or RV-A1B at MOI of 5 for 12 h.

Labeling and colocalization of MyrVP4 and TLRs. To label for fluorescence, 20 μg of MyrVP4 in 0.1 M sodium bicarbonate (pH 8.5) or DMSO were reacted with 100 μg of *N*-hydroxy succinimidyl (NHS) Cy3 (GE Healthcare Bio-Sciences, Pittsburgh PA) and purified on G-25 spin columns (GE Healthcare). Anti-VP4 and anti-CD14 were conjugated to NHS Cy3. Anti-TLR2 and anti-TLR4 (BioLegend, San Diego, CA) were labeled with NHS Cy5. Anti-myeloid differentiation primary response protein (MyD88; Santa Cruz Biotechnology, Dallas, TX) was conjugated to NHS Alexa Fluor 488.

To assess colocalization and specificity of MyrVP4-TLR2 interactions, Cy3-labeled MyrVP4 was added to cells on poly-D-lysine-coated slides or coverslips at a concentration of 100 ng/ml. Selected cells were also incubated with 200 ng/ml Cy5-labeled anti-TLR2 or Cy3-labeled anti-CD14. Cells were washed, fixed in 4% paraformaldehyde at 2–4°C for 13 h, stained with DAPI, and then mounted in 10% polyvinyl alcohol (59). In other experiments, cells were treated with blocking antibodies against TLR2 or VP4, IgG, or unlabeled MyrVP4 before fixation and processing for DAPI staining and immunofluorescence with labeled antibodies. Colocalization was visualized using a Zeiss Axioplan Apotome or Leica SP5 confocal microscope with FRET/fluorescence lifetime imaging capability (Microscopy and Image Analysis Core, University of Michigan). Colocalization was quantified using the National Institutes of Health ImageJ Fiji Coloc2 software plug-in and statistically summarized using Pearson's corre-

Table 1. *Clinical characteristics of children from whom bronchoalveolar macrophages were obtained*

Patient No.	Age, yr	Sex	Ethnicity	Race	Diagnosis
1	14	M	Hispanic	Caucasian	Cough, eosinophilia
2	12	M	Non-Hispanic	Caucasian	Premature birth, bronchiectasis, moderate persistent asthma
3	12	F	Hispanic	Mixed	Severe persistent asthma

lation coefficient (11). At least 4 separate images of ~20 cells each were quantified for each determination.

FRET photobleaching to assess MyrVP4-TLR2 interactions. The Cy3-Cy5 donor-acceptor pair was employed to assess FRET efficiency by acceptor photobleaching using a Leica inverted SP5 laser confocal microscope system and software package, as described elsewhere (56). Fixed cells processed for FRET did not include antifade reagent in the mounting medium. Photobleaching was performed with a supercontinuum white light laser tuned to 647 nm. Ten consecutive distinct areas of colocalization from four different experiments were chosen for quantification. Efficiency was expressed as a fraction of the difference between the donor fluorescence after and before bleaching and the fluorescence after bleaching: FRET efficiency was initially determined by the Leica FRET acceptor photobleaching protocol and corrected for donor photobleaching, cross talk of the acceptor photoproduct to the Cy3 channel, and partial Cy5 photobleaching. Images of pre- and postbleached areas were quantified using the National Institutes of Health ImageJ AccPBFRET plugin (45).

Other antibodies. The TLR2-neutralizing monoclonal antibody T2.5 (35) was obtained from BioLegend. Anti-polyhistidine was obtained from Sigma.

Cytokine responses to VP4. Recombinant VP4 or MyrVP4, synthetic MyrVP4, bacterial Lpp (each 100 ng), or carrier was incubated with 10 μg of IgG or anti-VP4 in 50 μl of PBS and added to 1 ml of cell culture medium, for a final concentration of 100 ng/ml. At this dilution, MyrVP4 rapidly binds to lipid membranes, where it is highly soluble (10, 43). For selected experiments, anti-TLR2 was added directly to the cell culture medium 1 h before MyrVP4 treatment. Selected samples were infected with RV-A1B at a MOI of 5.0. Virus was cultured in HeLa cells and partially purified by ultrafiltration, as described elsewhere (40). After 1 h, samples were transferred to 10% FBS-containing medium and, 18 h later, processed for mRNA transcript quantitation.

Quantitative PCR. After solubilization with TRIzol (Invitrogen), RNA was extracted from cells and tissue according to the manufacturer's recommendations. Purified RNA was processed for first-strand cDNA and quantitative PCR using reverse transcriptase and SYBR green quantitative PCR reagents (Thermo Fisher). Primers are described in Table 2. The resulting amplification and melt curves were analyzed to ensure specific PCR product. Threshold cycle (C_T) values were used to calculate the fold change in transcript levels compared with GAPDH using the $2^{-\Delta\Delta CT}$ method (48). The results were secondarily expressed as fold increase over sham.

RESULTS

MyrVP4 colocalizes with TLR2. After infection of 293/hTLR2 cells, RV-A1B colocalized with TLR2 within 5 min of treatment, as evidenced by colocalization of Cy3-conjugated anti-VP4 and Cy5-conjugated anti-TLR2 (Fig. 2*A*). As shown previously (37), RV infection tends to be variable, with not all cells showing the presence of virus by immunostaining. When 293/hTLR2 cells were treated for 5 min with 100 ng/ml Cy3-conjugated recombinant MyrVP4, we observed colocalization of VP4 and Cy5-conjugated anti-TLR2 (Fig. 2*B*). 293/hTLR2 cells treated with Cy3-conjugated synthetic MyrVP4 also showed colocalization of VP4 and Cy5-conjugated anti-TLR2 (Fig. 2*C*). There was no MyrVP4 binding or colocalization in 293/null cells that do not express TLR2 (Fig. 2*D*). Incubation with anti-VP4 or anti-TLR2 (10 μg/ml) 1 h before addition of Cy3-labeled MyrVP4 blocked binding of MyrVP4 and TLR2 (Fig. 2, *E* and *F*). Addition of excess unlabeled MyrVP4 lowered the intensity of binding (Fig. 2*G*). Labeled IgG did not bind to cells (not shown).

We also examined MyrVP4 and TLR2 fluorescence in cultured macrophages. Bone marrow-derived macrophages were isolated from wild-type and $TLR2^{-/-}$ mice. Wild-type cells treated with Cy3-labeled recombinant MyrVP4 and stained with anti-TLR2 showed colocalization (Fig. 2*H*), whereas $TLR2^{-/-}$ cells showed none (Fig. 2*I*). Finally, human bronchoalveolar macrophages incubated with Cy3-labeled recombinant MyrVP4 and fixed after 5 min also showed colocalization of VP4 with Cy5-labeled TLR2 at the cell surface (Fig. 2*J*). MyrVP4 was associated with both surface and intracellular TLR2, likely reflecting concentration in microdomains and endocytosis (13). Colocalization of RV-A1B and recombinant MyrVP4 with TLR2 in 293/hTLR2 cells, wild-type mouse bone marrow-derived macrophages, and human alveolar macrophages was quantified using Pearson's correlation coefficient, which, in each case, was significantly different from that of 293/null cells (Fig. 2*K*). In contrast, colocalization of MyrVP4 and TLR2 in $TLR2^{-/-}$ macrophages or 293/TLR2 cells treated with excess unlabeled anti-VP4, anti-TLR2, and recombinant MyrVP4 was close to zero.

Table 2. *Oligonucleotide primers*

Species	Gene	Sequence
Human	*CXCL1*	Forward: 5′-CACCCCAAGAAC-3′ Reverse: 5′- CACCAGTGAGCTTCCTCCTC-3′
Human	*CXCL2*	Forward: 5′-CAGCAATCCCCGGCTCCTGC-3′ Reverse: 5′-CAGTTCAGTGGCCAGGGGCG-3′
Human	*CXCL8*	Forward: 5′-TCTGCAGCT CTG TGT GAA GGT GCA GTT-3′ Reverse: 5′-AAC CCT CTG CAC CCA GTT TTC CT-3′
Human	*CXCL10*	Forward: 5′-TTGTCCACG TGT TGA GAT CAT-3′ Reverse: 5′-TTAGACCTT TCC TTG CTA ACT GC-3′
Human	*GAPDH*	Forward: 5′-CGACCACTTTGTCAAGCTCA-3′ Reverse: 5′-AGGGGTCTACATGGCAACTG-3′
Mouse	*Cxcl1*	Forward: 5′-TGC ACC CAA ACC GAA GAA GTC AT-3′ Reverse: 5′-CAA GGG AGC TTC AGG GTC AAG-3′
Mouse	*Cxcl2*	Forward: 5′-GCG CTG TCA ATG CCT GAA G-3′ Reverse: 5′-CGT CAC ACT CAA GCT CTG GAT-3′
Mouse	*Cxcl10*	Forward: 5′-GCT GCA ACT GCA TCC ATA TC-3′ Reverse: 5′-TTT CAT CGT GGC AAT GAT CT-3′
Mouse	*Gapdh*	Forward: 5′-GTC GGT GTG AAC GGA TTT G-3′ Reverse: 5′-GTC GTT GAT GGC AAC AAT CTC-3′

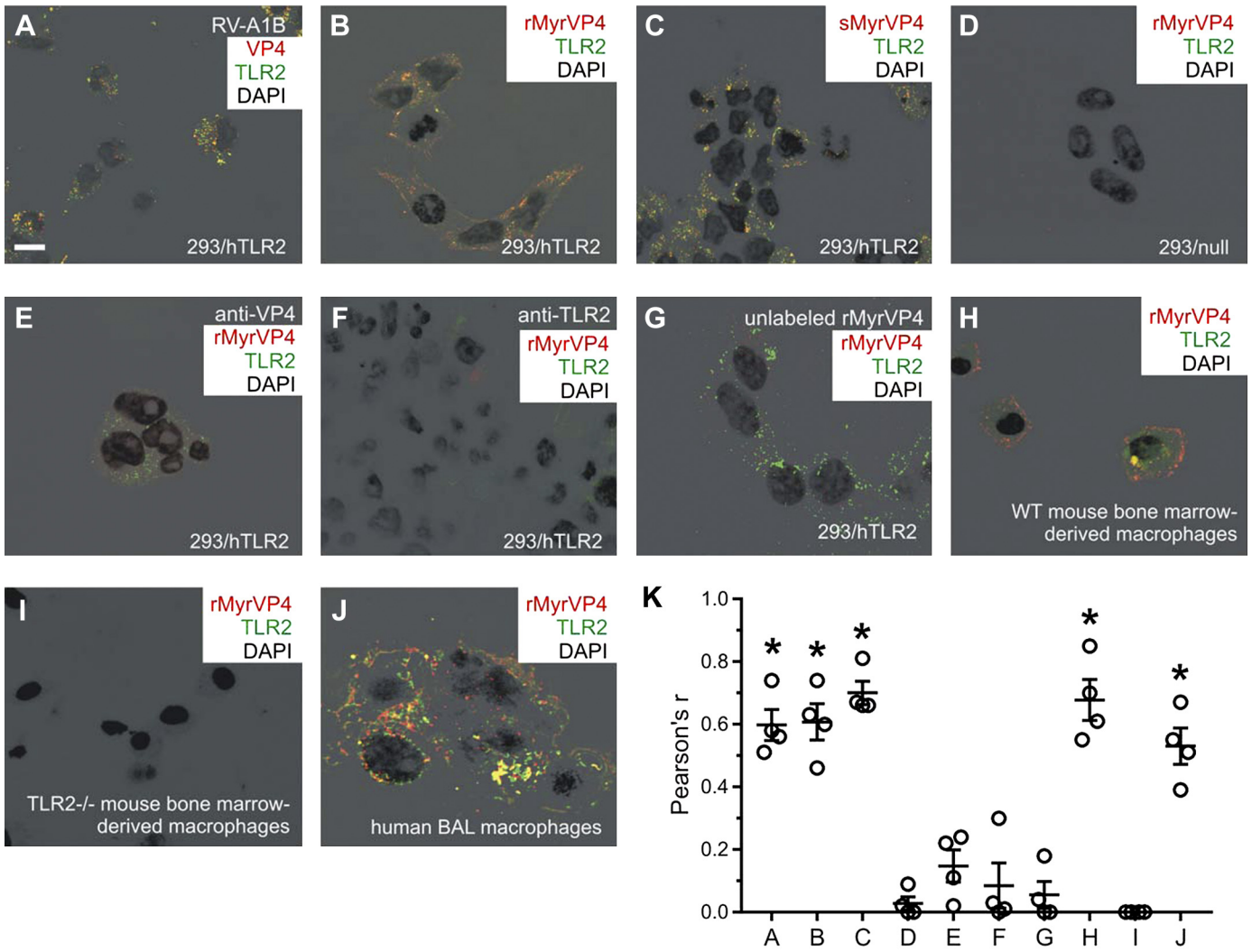

Fig. 2. Fluorescence microscopy demonstrating colocalization of rhinovirus (RV)-derived myristoylated (Myr) virus protein-4 (VP4) and Toll-like receptor 2 (TLR2). Live 293/hTLR2 (*A–C* and *E–G*) or 293/null (*D*) cells were treated for 5 min with RV-A1B (multiplicity of infection = 5; *A*) or 100 ng/ml Cy3-labeled recombinant (*B* and *D–J*) or synthetic (*C*) MyrVP4. Cells were stained with 200 ng/ml Cy3-labeled anti-VP4 (red channel) and 200 ng/ml Cy5-conjugated anti-TLR2 (green channel) before fixation. Scale bar = 10 μm. Confocal images were produced using a Leica SP5 laser confocal microscope. Orange-to-yellow VP4-TLR2 colocalization was noted in cells treated with RV (*A*), recombinant MyrVP4 (rMyrVP4, *B*), and synthetic MyrVP4 (sMyrVP4, *C*). No signal is visible in 293/null cells that do not express TLR2 (*D*) or in 293/hTLR2 cells preincubated with 10 μg of anti-VP4 (*E*), 10 μg of unlabeled anti-TLR2 (*F*), or 10 μM unlabeled rMyrVP4 (*G*). Wild-type (*H*) and TLR2$^{-/-}$ (*I*) bone marrow-derived macrophages were treated for 5 min with 100 ng/ml Cy3-labeled rMyrVP4 (red) and stained with 200 ng of Cy5-labeled anti-TLR2 (green). Colocalization is yellow-orange. No signal is visible in TLR2$^{-/-}$ cells. *J*: human bronchoalveolar (BAL) macrophages were treated for 5 min with 100 ng/ml Cy3-labeled rMyrVP4 (red) and stained with 200 ng/ml Cy5-labeled anti-TLR2 (green). Colocalization is yellow-orange. *K*: Cy3-labeled (VP4) and Cy5-labeled (TLR2) channels were quantified for correlation using Pearson's correlation coefficient (*r*). *x*-Axis labels correspond to treatments in *A–J*. Colocalization of either rMyrVP4 or sMyrVP4 and TLR2 was significantly greater in 293/hTLR2 cells, wild-type mouse macrophages, and human bronchoalveolar macrophages than 293/null cells (each $n = 4$). *$P < 0.0001$ vs. 293/null cells (by one-way ANOVA with Tukey's multiple-comparison test). IgG controls showed no colocalization (data not shown).

MyrVP4 induces colocalization of TLR2 with MyD88. After stimulation with pathogen, the adapter protein MyD88 is recruited close to the cell surface, where it colocalizes with its TLR (20, 50, 54). We examined colocalization of TLR2 and TLR4 following treatment of wild-type mouse bone marrow-derived macrophages with either MyrVP4 or LPS, a TLR4 ligand. Treatment with MyrVP4 induced aggregation of TLR2 and MyD88, whereas treatment with LPS did not (Fig. 3, *A–C*). Conversely, MyrVP4 failed to induce aggregation of TLR4 and MyD88, in contrast to LPS, which caused colocalization (Fig. 3, *D–F*). While there was some degree of basal MyD88 colocalization with both TLR2 and TLR4, MyrVP4 treatment significantly increased MyD88 colocalization with TLR2, but not TLR4 (Fig. 3*G*). LPS increased colocalization of MyD88 with TLR4, but not TLR2.

MyrVP4 specifically binds TLR2 as assessed by FRET. We assessed the capacity of Cy5-labeled anti-TLR2 photobleaching to increase Cy3-labeled MyrVP4 fluorescence intensity in 293/hTLR2 cells and bone marrow-derived macrophages from wild-type and TLR2$^{-/-}$ mice. A representative group of 293/hTLR2 cells exhibiting an increase in Cy3 fluorescence with Cy5 photobleaching is shown in Fig. 4*A*. Assessing 10 separate areas of colocalization per sample from 4 different experiments, we determined that, under the

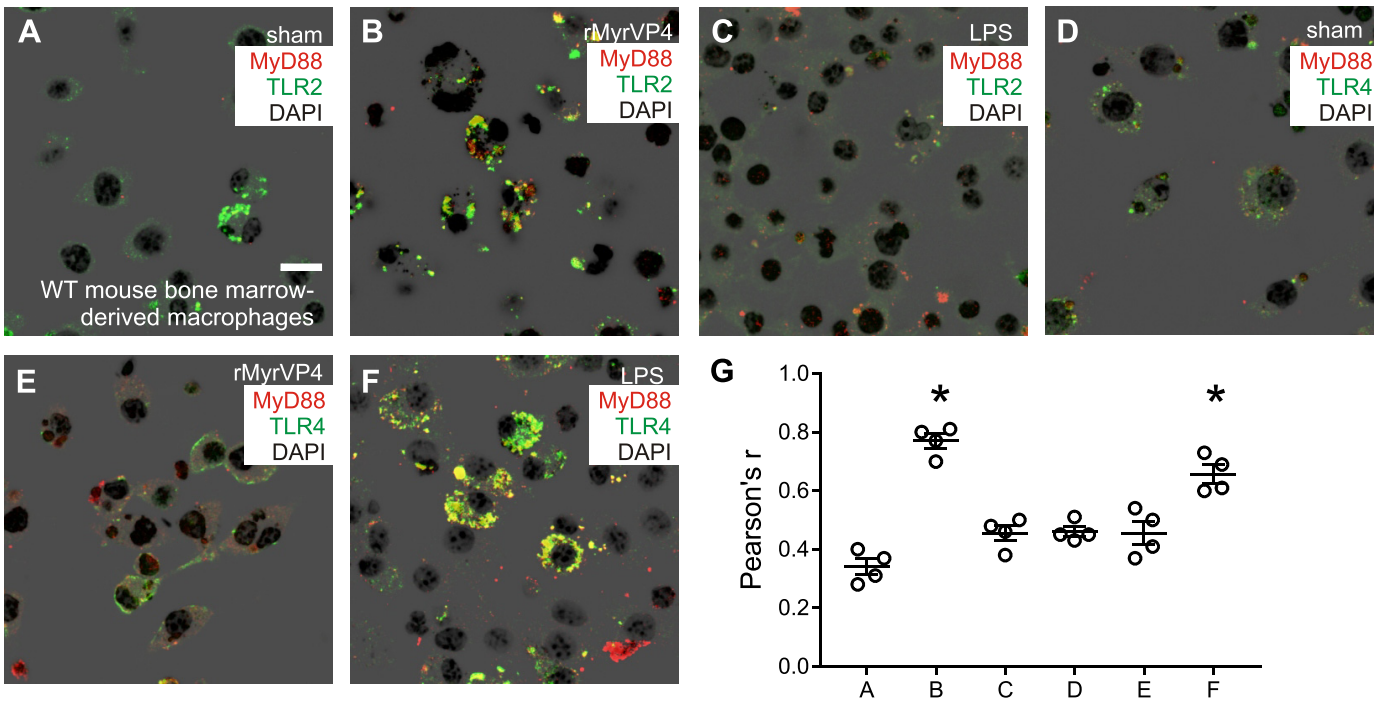

Fig. 3. Localization of myristoylated (Myr) virus protein-4 (VP4) with other Toll-like receptors (TLRs). Wild-type (WT) bone marrow-derived differentiated macrophages were treated with sham HeLa cell lysate (*A* and *D*), 100 ng/ml recombinant MyrVP4 (rMyrVP4, *B* and *E*), or 100 ng/ml LPS (*C* and *F*) for 5 min. Cells were stained with Alexa Fluor 488-conjugated anti-MyD88 (red) and either Cy5-conjugated anti-TLR2 (green; *A–C*) or Cy5-conjugated anti-TLR4 (green; *D–F*). MyD88 and TLR colocalize as yellow. *G*: treatment with rMyrVP4, but not LPS, significantly initiates colocalization of MyD88 and TLR2. In contrast, treatment with LPS, but not rMyrVP4, induces colocalization of MyD88 and TLR4. Colocalization signals were quantified for correlation using Pearson's correlation coefficient (*r*). *x*-Axis labels correspond to treatments in *A–F* ($n = 4$). *$P < 0.0001$ vs. sham-treated cells (by one-way ANOVA with Tukey's multiple-comparison test).

specified conditions, the Cy3-labeled MyrVP4-Cy5-labeled anti-TLR2 interaction had an average fractional FRET efficiency of 0.245 ± 0.024 (mean ± SE) (Fig. 4*B*), indicating that Cy3-labeled MyrVP4 and Cy5-labeled anti-TLR2 are closely associated. Addition of unlabeled MyrVP4 lowered FRET efficiency, as did blocking the TLR2 receptor with excess unlabeled anti-TLR2 or sequestration of MyrVP4 by neutralizing anti-VP4 antibody (Fig. 4*B*). At any given concentration, FRET efficiency was constant over the range of sampled fluorescence intensities (data not shown), but FRET efficiency saturated as the concentration of Cy5-labeled anti-TLR2 increased (Fig. 4*C*).

Cy3-labeled MyrVP4 and Cy5-labeled anti-TLR2 also colocalized and showed FRET exchange in bone marrow-derived macrophages from wild-type, but not TLR2$^{-/-}$, mice (Fig. 4*D*). Finally, we investigated potential interactions with CD14, which associates with TLR2 in lipid microdomain signaling complexes (56). CD14 colocalizes with TLR2 in wild-type bone marrow-derived macrophages but demonstrates FRET only in the presence of unlabeled MyrVP4 (Fig. 4, *D* and *E*). FRET efficiency between anti-CD14 and anti-TLR2 increases and saturates upon addition of unlabeled MyrVP4.

VP4 and MyrVP4 stimulate chemokine transcription and are neutralized by anti-VP4. Purified recombinant VP4 and VP4 prepared from bacteria grown in the presence of pNMT-1 and myristic acid (MyrVP4) activated chemokine (C-X-C motif) ligand (CXCL)-8 production in 293/hTLR2, but not 293/null, cells (Fig. 5*A*). The CXCL8 response to MyrVP4 was significantly greater than to VP4.

Both VP4 and MyrVP4 signals were sensitive to preincubation with anti-VP4. In contrast, bacterial Lpp protein

Fig. 4. Myristoylated (Myr) virus protein-4 (VP4) forms a close association with Toll-like receptor 2 (TLR2) in 293/hTLR2 cells and macrophages. *A–C*: confocal Cy3-labeled MyrVP4 (Cy3-MyrVP4) fluorescence resonance energy transfer (FRET) to Cy5-labeled anti-TLR2 (Cy5-anti-TLR2) was assessed by laser photobleaching. *A*: 293/hTLR2 cells bound with 10 ng of Cy3-MyrVP4 (red) and Cy5-anti-TLR2 (green) (*left*). DAPI staining of nuclei is an underlay in black. FRET is shown as blue (*middle*). Colocalization of MyrVP4 and TLR2 is light blue to white (*right*). *B*: FRET efficiency of Cy3-MyrVP4-Cy5-anti-TLR2 interaction in 293/hTLR2 cells. Unlabeled MyrVP4 competes with Cy3-MyrVP4 binding to anti-TLR2. Values are means ± SE; $n = 4$, with each data point representing the mean of 10 bleached regions per individual experiment. *$P < 0.05$ vs. Cy3-IgG or Cy5-IgG alone (by one-way ANOVA with Tukey's multiple-comparison test). *C*: FRET efficiency of Cy3-MyrVP4-Cy5-anti-TLR2 interaction in 293/hTLR2 (TLR2$^+$) and 293/null (TLR2$^-$) cells. FRET efficiency increases as further Cy5-anti-TLR2 acceptor is added. (Values are means ± SE; $n = 4$. *$P < 0.05$ vs. Cy5-IgG, by one-way ANOVA.) *D* and *E*: FRET in mouse bone marrow-derived macrophages. *D*: FRET efficiency of Cy3-MyrVP4-Cy5-anti-TLR2 interaction in macrophages from wild-type (TLR2$^+$) and TLR2-null (TLR2−) mice (*columns 1* and *2*); MyrVP4 binds TLR2 in macrophages derived from TLR2$^+$, but not TLR2−, mice. FRET efficiency of Cy3-anti-CD14 (100 ng)-Cy5-anti-TLR2 interaction increases with escalating doses of unlabeled MyrVP4 (*columns 3–9*). Values are means ± SE; $n = 4$. *$P < 0.05$ vs. Cy3-IgG or Cy5-IgG (by one-way ANOVA). *E*: MyrVP4 recruits CD14 to TLR2. When Cy3 is coupled to anti-CD14, there is colocalization with Cy5 anti-TLR2, and increasing MyrVP4 further increases FRET efficiency (blue; colocalized FRET appears white).

stimulated a lower level of CXCL8 mRNA expression, which was insensitive to anti-VP4, suggesting that MyrVP4-induced CXCL8 mRNA expression was not due to contamination by Lpp. In another set of experiments, synthetic MyrVP4 generated TLR2-dependent CXCL8 mRNA expression, which was analogous to that produced by recombinant MyrVP4 and neutralized by the VP4 antibody (Fig. 5*B*).

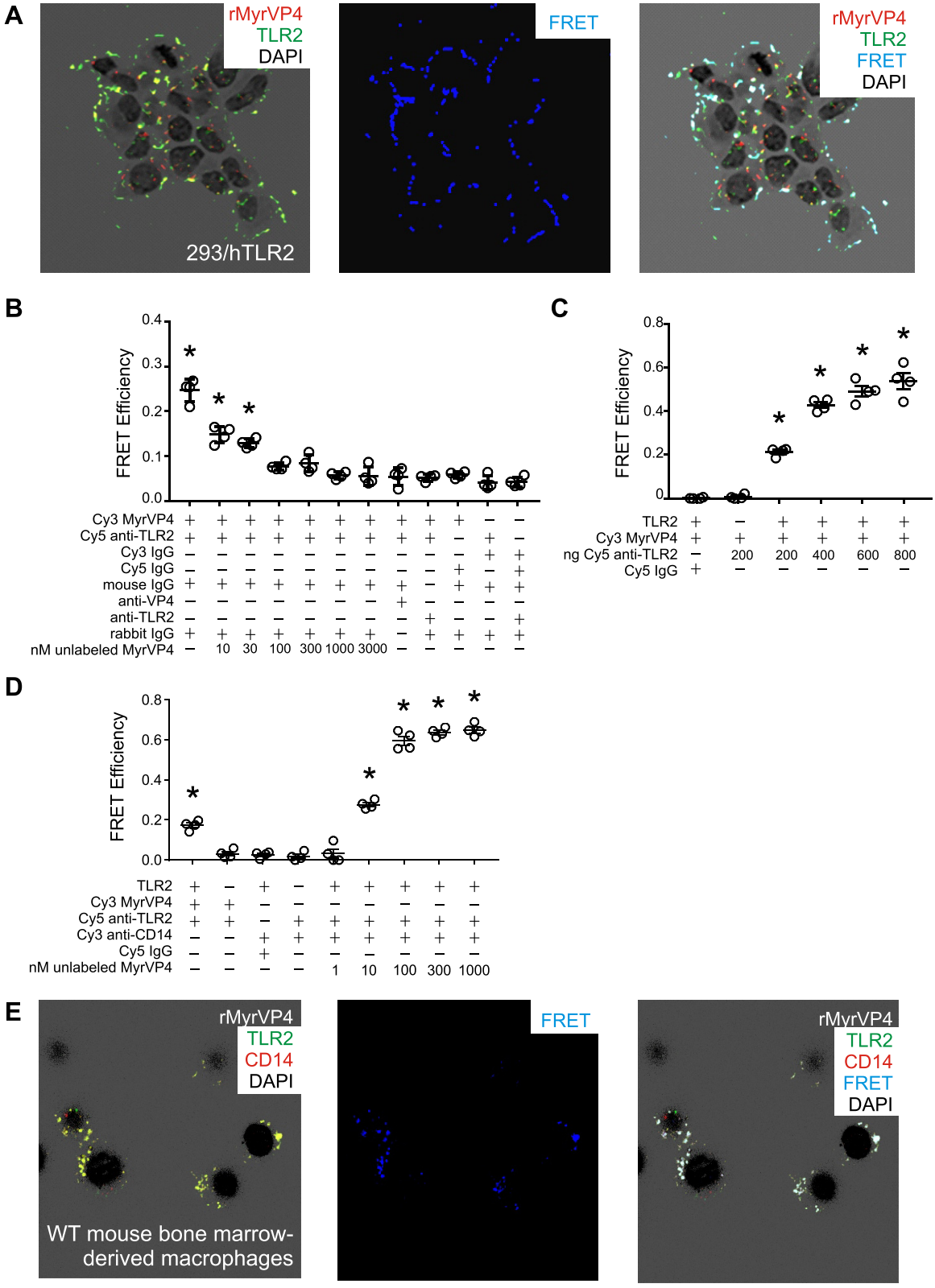

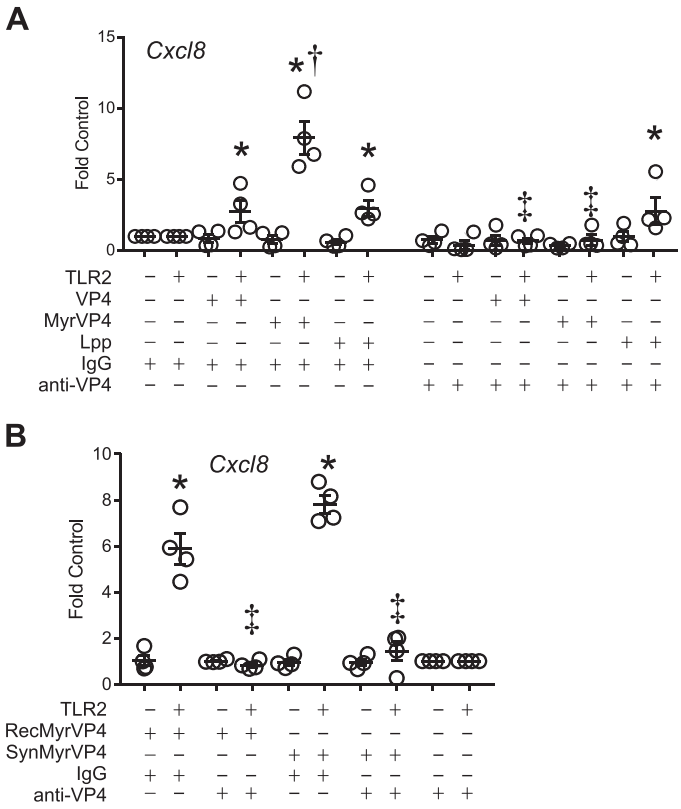

Fig. 5. Myristoylated (Myr) virus protein-4 (VP4) induces chemokine (C-X-C motif) ligand (CXCL)-8 mRNA expression in 293/hTLR2 cells. *A*: 100 ng of recombinant VP4 (MyrVP4) or 100 ng of bacterial murein lipoprotein (Lpp) were incubated with 10 μg of IgG or anti-VP4 and added to 293/hTLR2 or 293/null cells in serum-free medium for 1 h, after which serum-free medium was replaced with serum-containing medium. After 18 h, samples were processed for CXCL8 and GAPDH mRNA transcript analysis by quantitative PCR. Data are depicted as fold increase from sham ($n = 4$, with each data point representing the mean of 2–3 replicates per individual experiment). *$P < 0.05$ vs. solvent control, †$P < 0.05$ vs. VP4 and Lpp, ‡$P < 0.05$ vs. IgG controls (by one-way ANOVA with Tukey's multiple-comparison test). *B*: 100 ng of recombinant MyrVP4 (RecMyrVP4) or 100 ng of synthetic MyrVP4 (SynMyrVP4) were incubated with IgG or anti-VP4 and added to 293/hTLR2 or 293/null cells, as described in *A*. After 18 h, samples were processed for CXCL8 and GAPDH mRNA transcript analysis by quantitative PCR. Data are expressed as fold increase from sham ($n = 4$). *$P < 0.05$ vs. solvent controls, ‡$P < 0.05$ vs. IgG controls (by one-way ANOVA with Tukey's multiple-comparison test).

MyrVP4 induces TLR2-dependent cytokine mRNA expression in macrophages. We examined macrophage CXCL1, CXCL2, and CXCL10 expression in response to MyrVP4. These chemokines are produced by macrophages after RV infection (24, 28, 47, 63) and are important for neutrophilic and lymphocytic inflammation following infection (39). RV-A1B and MyrVP4 significantly increased CXCL1, CXCL2, and CXCL8 mRNA expression in human alveolar macrophages, whereas only RV-A1B increased CXCL10 mRNA expression over sham (Fig. 6*A*). Mouse alveolar macrophages from TLR2-expressing wild-type mice incubated with MyrVP4 showed significant increases in CXCL1, CXCL2, and CXCL10 mRNA expression (Fig. 6*B*). Human and mouse macrophages showed smaller responses to nonmyristoylated VP4, and alveolar macrophages from TLR2$^{-/-}$ mice showed no response to either recombinant protein or RV-A1B. As shown previously (14), intact RV increased chemokine mRNA expression without adversely affecting macrophage viability.

Native RV-derived MyrVP4 binds epithelial cells to stimulate cytokine transcription. Sham-treated BEAS-2B cells showed cytoplasmic TLR2 expression (Fig. 7*A*). As shown with intact RV-A1B (Fig. 7*B*), RV-MyrVP4-bound TLR2 (Fig. 7*C*) was competed off with unlabeled TLR2 antibody (Fig. 7*D*). Intact RV-A1B, RV-MyrVP4, recombinant MyrVP4, and synthetic MyrVP4 each stimulated CXCL1, CXCL2, and CXCL8 transcription in this transformed bronchial cell line (Fig. 7*E*). As in macrophages, none of the peptides stimulated significant transcription of CXCL10. Finally, primary human bronchial epithelial cells were isolated and mucociliary-differentiated in culture (Fig. 7*F*). Again, RV-A1B and RV-MyrVP4 rapidly bound to TLR2, and unlabeled anti-TLR2 blocked colocalization. As in BEAS-2B cells, RV-A1B and RV-MyrVP4 increased CXCL1, CXCL2, and CXCL8 transcription in primary differentiated human bronchial epithelial cells (Fig. 7*G*). Only RV-A1B increased CXCL10 transcription.

DISCUSSION

Recent studies have uncovered a potential role for TLR2 in the sensing of RV infection. TLR2 is required and sufficient for RV-induced NF-κB activation in cultured airway epithelial cells and HEK cells, respectively (53). TLR2 inhibition also blocked responses to replication-deficient UV-irradiated virus. Similarly, we found that RV-induced cytokine expression and viral attachment were abolished in bone marrow-derived macrophages from TLR2$^{-/-}$ mice (47) and that TLR2-dependent cytokine expression did not depend on viral endocytosis or replication. We also colocalized RV and TLR2 on the macrophage cell surface. Finally, we found that TLR2 is required for RV-induced airway inflammation in naïve and allergen-treated mice and that transfer of wild-type, IL-4-treated bone-marrow derived macrophages to TLR2$^{-/-}$ mice is sufficient for RV-induced airway eosinophilic inflammation, mucous metaplasia, and airway hyperresponsiveness (17). At first blush, an interaction between TLR2 and the RV capsid is surprising, since picornaviruses are nonenveloped and their capsid does not include a lipid component. We hypothesized that VP4, an internal capsid protein that is myristoylated upon viral replication (8, 10) and externalized upon viral binding (31), is a ligand for TLR2. We found that recombinant MyrVP4 and TLR2 colocalize and that colocalization was blocked by anti-TLR2 and anti-VP4. MyrVP4-induced chemokine expression was higher than that elicited by VP4 alone and was attenuated by anti-TLR2 and anti-VP4. Expression was similarly increased by synthetic MyrVP4 and MyrVP4 purified from RV-A1B-infected HeLa cells. Cy3-labeled MyrVP4 and Cy5-labeled anti-TLR2 showed an average fractional FRET efficiency of ~25%, suggesting that TLR2 and VP4 are positioned within a distance of ~50 Å (25, 46). Together, these results suggest that MyrVP4 and TLR2 interact to generate a proinflammatory response in RV-infected cells.

We used a bacterial expression system to express VP4 and MyrVP4 proteins as ligands for TLR2 interaction studies. Myristoylation was accomplished by cotransformation of BL21(DE3) pLysS with plasmids encoding VP4 and NMT-1 in the presence of myristic acid. Use of a bacterial expression system raises the possibility that the proinflammatory effects of

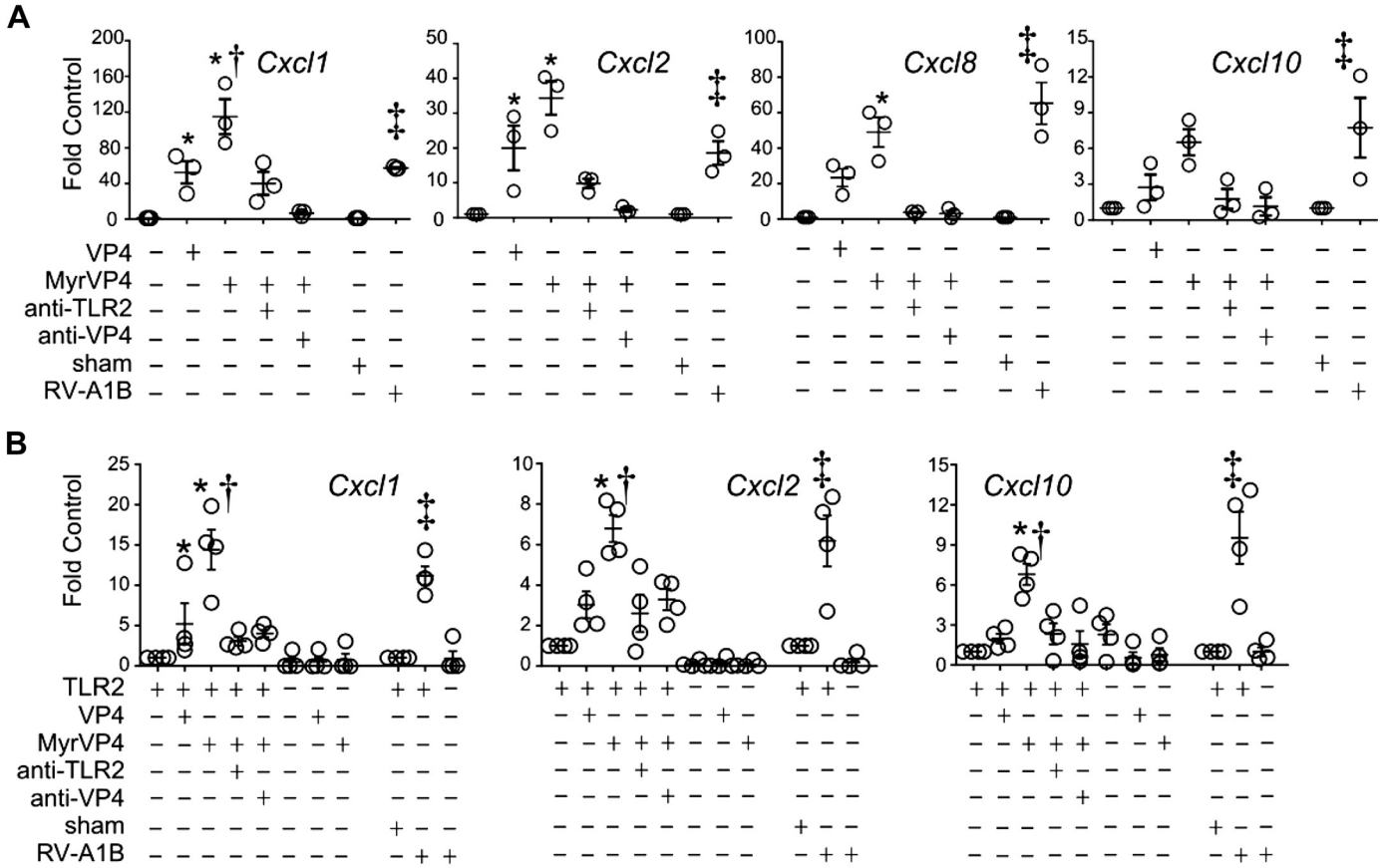

Fig. 6. Myristoylated (Myr) virus protein-4 (VP4) elicits Toll-like receptor 2 (TLR2)-dependent chemokine responses in macrophages. *A*: human alveolar macrophages were treated with VP4 or MyrVP4 and preincubated with IgG, anti-TLR2, or anti-VP4. For comparison, cells were also treated with intact rhinovirus (RV)-A1B. Cells were harvested for mRNA transcript analysis by quantitative PCR. MyrVP4 significantly increased CXCL1, CXCL2, and CXCL8 mRNA expression. After normalization to GAPDH, data were expressed as fold increase from sham ($n = 3$, with each data point representing the mean of 2–3 replicates per individual experiment). *$P < 0.05$ vs. solvent control, †$P < 0.05$ vs. VP4, ‡$P < 0.05$ vs. sham alone (by one-way ANOVA with Tukey's multiple-comparison test). *B*: mouse alveolar macrophages from wild-type, but not TLR2-null, mice express chemokines in response to MyrVP4 and Cy3-labeled MyrVP4. For comparison, cells were also treated with intact RV-A1B. After normalization to GAPDH, data were expressed as fold increase from sham ($n = 4$). *$P < 0.05$ vs. solvent and IgG control, †$P < 0.05$ vs. VP4, ‡$P < 0.05$ vs. sham alone (by one-way ANOVA with Tukey's multiple-comparison test).

recombinant MyrVP4 are caused by contamination with bacterial products, not by MyrVP4 itself. Aside from the protein of interest, the second most abundant constituent was Lpp (also called Braun's lipoprotein), a peptidoglycan-conjugated lipoprotein of the *E. coli* outer membrane. However, significantly less chemokine expression was induced by incubation of cells with purified Lpp than MyrVP4. Furthermore, incubation of cells with a preparation of MyrVP4 produced by chemical peptide synthesis and a third preparation purified from RV-A1B-infected HeLa cells induced levels of chemokine expression similar to that induced by recombinant VP4. The MyrVP4 signal was blocked with anti-VP4, further evidence against nonspecific TLR2 activation by bacterial products.

Cy3-labeled MyrVP4 and Cy5-labeled anti-TLR2 showed an average fractional FRET efficiency of ~25%, with Cy5-labeled anti-TLR2 increasing and unlabeled MyrVP4 decreasing FRET efficiency. FRET was not present in $TLR2^{-/-}$ cells. Together, these results suggest that MyrVP4 and TLR2 are in close physical proximity. FRET has been used previously to detect recognition of a fluorescence-labeled bacterial lipopeptide by TLR2 (58). Although our FRET studies indicate that TLR2 and VP4 are positioned within a distance of 50 Å, we did not precisely characterize the nature of this interaction. TLR2 is a membrane surface receptor that recognizes bacterial lipopeptides and lipoteichoic acid. Cellular activation after TLR2 ligation depends on two main factors: *1*) the type of TLR2 ligand and *2*) cellular expression of additional TLR2 coreceptors, including TLR1, TLR6, CD14, and CD36. Studies employing synthetic compounds suggest that the ideal ligand for TLR2 receptor activity is a Cys-Ser/Thr/Gly/Ala lipopeptide containing at least one ester-bound fatty acid acyl group of optimal length (C_{14}–C_{20}) (6). Shorter ester-bound fatty acids and amide-bound fatty acids of any size tended to have reduced TLR2-mediated effects. For the TLR2 ligand Pam_3CSK_4, the two glycerol-bound palmitoyl chains dock with the hydrophobic pocket of TLR2, while the third amide-bound lipid chain docks with the TLR1 channel, stabilizing the TLR2/1 heterodimer (22). Lipid modification of VP4 might allow loose binding to the hydrophobic pocket of TLR2. Although the myristyl group is bound to the VP4 polypeptide through an amide bond, the intensely hydrophobic peptide backbone might allow VP4 to come into close proximity with TLR2 in the cell membrane, increasing the effective concentration available for TLR2 activation. In our studies we found evi-

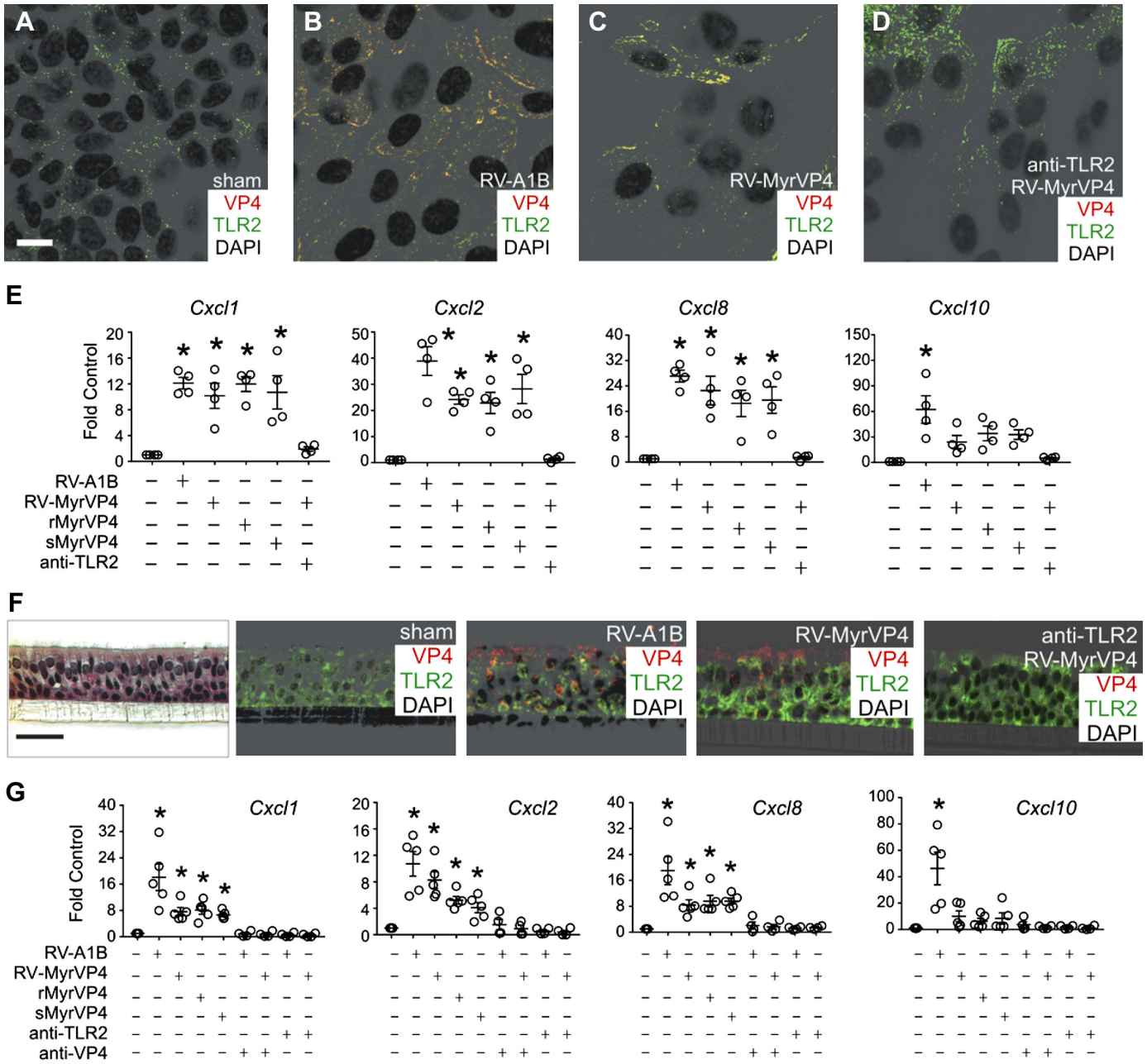

Fig. 7. Rhinovirus (RV)-derived myristoylated (Myr) virus protein-4 (VP4) binds to epithelial cells and stimulates chemokine transcription. RV-MyrVP4 was purified by urea solubilization and anti-VP4 affinity chromatography (see MATERIALS AND METHODS). *A–D*: Beas-2B cells were treated with sham HeLa cell lysate (*A*), RV-A1B (*B*), or RV-MyrVP4 (*C* and *D*). Selected cells were preincubated with unlabeled 10 μg/ml anti-Toll-like receptor 2 (TLR2). Fixed cells were stained with Cy3-labeled anti-VP4 (red) and Cy5-labeled anti-TLR2 (green). Colocalization is yellow. Scale bar = 50 μm. *E*: RV-A1B (multiplicity of infection = 5), RV-MyrVP4, recombinant MyrVP4 (rMyrVP4), and synthetic MyrVP4 (sMyrVP4) (each at 100 ng/ml) significantly increase CXCL1, CXCL2, and CXCL8 transcription in Beas-2B cells, but only RV-A1B significantly increases CXCL10 ($n = 4$). *$P < 0.05$ vs. solvent and IgG control (by ANOVA and Tukey's multiple-comparison test). *F*: primary human bronchial epithelial cells cultured on Transwell membranes. Cells develop cilia, as assessed by hematoxylin-and-eosin staining (*far left*). Scale bar = 50 μm. Cells were stained with Cy5-conjugated anti-TLR2 (green) and Cy3-conjugated anti-VP4 (red). Cells infected with RV-A1B or treated with 100 ng of MyrVP4 show colocalization of VP4 and TLR2 (orange-yellow). Colocalization is blocked by preincubation with anti-TLR2 (*right*). *G*: human bronchial epithelial cells differentiated at air-liquid interface were incubated with RV-A1B (multiplicity of infection = 5), RV-MyrVP4, rMyrVP4, or sMyrVP4 (100 ng/ml) for 12 h. All 4 treatments significantly elevated transcription of CXCL1, CXCL2, and CXCL8, but only RV-A1B increased CXCL10 transcription ($n = 4$ experiments using 1 epithelial cell isolate). *$P < 0.05$ vs. solvent and IgG control (by one-way ANOVA with Tukey's multiple-comparison test).

dence for TLR2 colocalization and binding with CD14. CD14 (but not TLR2) is also required for influenza A-induced cytokine production in human and mouse macrophages (44).

Alternatively, VP4 is likely to come into close contact with TLR2 in lipid rafts. TLR2 and its coreceptors have been localized to lipid rafts (30, 32, 54–57), and we have shown in human bronchial epithelial cells that RV-A39 colocalizes with Src, p85α and p110β phosphoinositide 3-kinase, and Akt in lipid rafts (1). The polar lipids in lipid rafts are predominantly acylated by saturated fatty acids, unlike phospholipids in non-

lipid raft membranes, which are acylated by polyunsaturated fatty acids, suggesting that saturated fatty acyl chains (e.g., myristic acid) favor lipid raft association (21).

As noted above, we found that MyrVP4-induced chemokine expression was higher than that elicited by VP4 alone. These data suggest that MyrVP4 is sufficient for RV-induced cytokine expression. Cytokine expression was absent in TLR2$^{-/-}$ cells, demonstrating a requirement of TLR2 for MyrVP4 -induced cytokine responses. However, VP4 is also likely to have TLR2-independent effects. VP4 has the intrinsic ability to bind lipid membranes, resulting in their permeabilization (10). VP4 is directly involved in mediating membrane penetration during cell entry (5). Studies utilizing recombinant His-tagged VP4 have shown that VP4 interacts with membranes to make them permeable by formation of multimeric, size-selective membrane pores with properties consistent with the transport of viral genome through the membrane (43). Myristoylation is required for membrane targeting and permeability (33, 43) and significantly improves pore formation by increasing the efficiency of the initial membrane interaction. It should also be noted that whereas VP4 treatment was sufficient for mRNA expression of CXCL1, CXCL2, and CXCL8, it failed to induce CXCL10 transcription. These data are consistent with the notion that binding and/or endocytosis of RV may be sufficient, and viral replication may be unnecessary, for a subset of initial cytokine responses (16, 40, 52), to be followed by a second set of replication-dependent responses.

We found colocalization of TLR2 and VP4, as well as VP4-mediated cytokine expression, in both macrophages and airway epithelial cells. Our focus on macrophages was based on recent data suggesting that while epithelial cells are indeed the main site of RV replication, macrophages and other immune cells are the main source of cytokine production after infection (2, 7, 19, 23, 26, 27, 36, 38, 41).

There is evidence that genetic differences in TLR2 expression influence the development of asthma. Significantly higher expression of CD14 and TLR2 was reported in peripheral blood monocytes from farmers' children with reduced risk of atopy than from non-farmers' children (29). Later, a T allele (genotype AT or TT) of the TLR2/−16934 polymorphism was associated with reduced risk of asthma in children of farmers (12). A T allele of the −16934 polymorphism has also been associated with decreased wheezing and bronchial hyperresponsiveness in children who attend day care (9). Since TLR2/−16934 is a marker for a group of highly linked TLR2 single-nucleotide polymorphisms, the functional explanation for these associations is unclear. However, since viral infections play a role in the development of asthma and atopy (reviewed in Ref. 34), binding of MyrVP4 to TLR2 could play a role in this association.

In conclusion, we have found a specific interaction between MyrVP4 and TLR2 that generates a proinflammatory response. This observation opens the door for therapeutic intervention, for example, desensitization of TLR2, or use of anti-VP4 antibodies. Further characterization of the VP4-TLR2 interaction, for example, by X-ray crystallography, may allow more specific interventions.

ACKNOWLEDGMENTS

We acknowledge the Proteomics and Imaging Cores at the University of Michigan.

GRANTS

This work was supported by National Heart, Lung, and Blood Institute Grant R01 HL-134369 (M. B. Hershenson).

DISCLAIMERS

The funders had no role in study design, data collection and analysis, decision to publish, or preparation of the manuscript.

DISCLOSURES

No conflicts of interest, financial or otherwise, are declared by the authors.

AUTHOR CONTRIBUTIONS

J.K.B. and M.B.H. conceived and designed research; J.K.B., M.H., S.J., J.L.H., J.L., T.I., A.M.G., and C.R. performed experiments; J.K.B. and M.B.H. analyzed data; J.K.B. and M.B.H. interpreted results of experiments; J.K.B. and M.B.H. prepared figures; J.K.B. and M.B.H. drafted manuscript; J.K.B. and M.B.H. edited and revised manuscript; J.K.B. and M.B.H. approved final version of manuscript.

REFERENCES

1. **Bentley JK, Newcomb DC, Goldsmith AM, Jia Y, Sajjan US, Hershenson MB.** Rhinovirus activates interleukin-8 expression via a Src/p110β phosphatidylinositol 3-kinase/Akt pathway in human airway epithelial cells. *J Virol* 81: 1186–1194, 2007. doi:10.1128/JVI.02309-06.
2. **Bentley JK, Sajjan US, Dzaman MB, Jarjour NN, Lee WM, Gern JE, Hershenson MB.** Rhinovirus colocalizes with CD68- and CD11b-positive macrophages following experimental infection in humans. *J Allergy Clin Immunol* 132: 758–761.e3, 2013. doi:10.1016/j.jaci.2013.04.020.
3. **Bochkov YA, Watters K, Ashraf S, Griggs TF, Devries MK, Jackson DJ, Palmenberg AC, Gern JE.** Cadherin-related family member 3, a childhood asthma susceptibility gene product, mediates rhinovirus C binding and replication. *Proc Natl Acad Sci USA* 112: 5485–5490, 2015. doi:10.1073/pnas.1421178112.
4. **Braun V, Rehn K.** Chemical characterization, spatial distribution and function of a lipoprotein (murein-lipoprotein) of the *E. coli* cell wall. The specific effect of trypsin on the membrane structure. *Eur J Biochem* 10: 426–438, 1969. doi:10.1111/j.1432-1033.1969.tb00707.x.
5. **Bubeck D, Filman DJ, Cheng N, Steven AC, Hogle JM, Belnap DM.** The structure of the poliovirus 135S cell entry intermediate at 10-angstrom resolution reveals the location of an externalized polypeptide that binds to membranes. *J Virol* 79: 7745–7755, 2005. doi:10.1128/JVI.79.12.7745-7755.2005.
6. **Buwitt-Beckmann U, Heine H, Wiesmüller K-H, Jung G, Brock R, Ulmer AJ.** Lipopeptide structure determines TLR2 dependent cell activation level. *FEBS J* 272: 6354–6364, 2005. doi:10.1111/j.1742-4658.2005.05029.x.
7. **Chairakaki AD, Saridaki MI, Pyrillou K, Mouratis MA, Koltsida O, Walton RP, Bartlett NW, Stavropoulos A, Boon L, Rovina N, Papadopoulos NG, Johnston SL, Andreakos E.** Plasmacytoid dendritic cells drive acute asthma exacerbations. *J Allergy Clin Immunol* 142: 542–556.e12, 2018. doi:10.1016/j.jaci.2017.08.032.
8. **Chow M, Newman JFE, Filman D, Hogle JM, Rowlands DJ, Brown F.** Myristylation of picornavirus capsid protein VP4 and its structural significance. *Nature* 327: 482–486, 1987. doi:10.1038/327482a0.
9. **Custovic A, Rothers J, Stern D, Simpson A, Woodcock A, Wright AL, Nicolaou NC, Hankinson J, Halonen M, Martinez FD.** Effect of day care attendance on sensitization and atopic wheezing differs by Toll-like receptor 2 genotype in 2 population-based birth cohort studies. *J Allergy Clin Immunol* 127: 390–397.e9, 2011. doi:10.1016/j.jaci.2010.10.050.
10. **Davis MP, Bottley G, Beales LP, Killington RA, Rowlands DJ, Tuthill TJ.** Recombinant VP4 of human rhinovirus induces permeability in model membranes. *J Virol* 82: 4169–4174, 2008. doi:10.1128/JVI.01070-07.
11. **Dunn KW, Kamocka MM, McDonald JH.** A practical guide to evaluating colocalization in biological microscopy. *Am J Physiol Cell Physiol* 300: C723–C742, 2011. doi:10.1152/ajpcell.00462.2010.
12. **Eder W, Klimecki W, Yu L, von Mutius E, Riedler J, Braun-Fahrländer C, Nowak D, Martinez FD; ALEX Study Team.** Toll-like receptor 2 as a major gene for asthma in children of European farmers. *J Allergy Clin Immunol* 113: 482–488, 2004. doi:10.1016/j.jaci.2003.12.374.

13. **Ganjian H, Zietz C, Mechtcheriakova D, Blaas D, Fuchs R.** ICAM-1 binding rhinoviruses enter HeLa cells via multiple pathways and travel to distinct intracellular compartments for uncoating. *Viruses* 9: 68, 2017. doi:10.3390/v9040068.
14. **Gern JE, Dick EC, Lee WM, Murray S, Meyer K, Handzel ZT, Busse WW.** Rhinovirus enters but does not replicate inside monocytes and airway macrophages. *J Immunol* 156: 621–627, 1996.
15. **Greve JM, Davis G, Meyer AM, Forte CP, Yost SC, Marlor CW, Kamarck ME, McClelland A.** The major human rhinovirus receptor is ICAM-1. *Cell* 56: 839–847, 1989. doi:10.1016/0092-8674(89)90688-0.
16. **Griego SD, Weston CB, Adams JL, Tal-Singer R, Dillon SB.** Role of p38 mitogen-activated protein kinase in rhinovirus-induced cytokine production by bronchial epithelial cells. *J Immunol* 165: 5211–5220, 2000. doi:10.4049/jimmunol.165.9.5211.
17. **Han M, Chung Y, Young Hong J, Rajput C, Lei J, Hinde JL, Chen Q, Weng SP, Bentley JK, Hershenson MB.** Toll-like receptor 2-expressing macrophages are required and sufficient for rhinovirus-induced airway inflammation. *J Allergy Clin Immunol* 138: 1619–1630, 2016. doi:10.1016/j.jaci.2016.01.037.
18. **Hofer F, Gruenberger M, Kowalski H, Machat H, Huettinger M, Kuechler E, Blass D.** Members of the low density lipoprotein receptor family mediate cell entry of a minor-group common cold virus. *Proc Natl Acad Sci USA* 91: 1839–1842, 1994. doi:10.1073/pnas.91.5.1839.
19. **Hong JY, Bentley JK, Chung Y, Lei J, Steenrod JM, Chen Q, Sajjan US, Hershenson MB.** Neonatal rhinovirus induces mucous metaplasia and airways hyperresponsiveness through IL-25 and type 2 innate lymphoid cells. *J Allergy Clin Immunol* 134: 429–439.e8, 2014. doi:10.1016/j.jaci.2014.04.020.
20. **Hornef MW, Normark BH, Vandewalle A, Normark S.** Intracellular recognition of lipopolysaccharide by toll-like receptor 4 in intestinal epithelial cells. *J Exp Med* 198: 1225–1235, 2003. doi:10.1084/jem.20022194.
21. **Huang S, Rutkowsky JM, Snodgrass RG, Ono-Moore KD, Schneider DA, Newman JW, Adams SH, Hwang DH.** Saturated fatty acids activate TLR-mediated proinflammatory signaling pathways. *J Lipid Res* 53: 2002–2013, 2012. doi:10.1194/jlr.D029546.
22. **Jin MS, Kim SE, Heo JY, Lee ME, Kim HM, Paik SG, Lee H, Lee JO.** Crystal structure of the TLR1-TLR2 heterodimer induced by binding of a tri-acylated lipopeptide. *Cell* 130: 1071–1082, 2007. doi:10.1016/j.cell.2007.09.008.
23. **Juno JA, Keynan Y, Fowke KR.** Invariant NKT cells: regulation and function during viral infection. *PLoS Pathog* 8: e1002838, 2012. doi:10.1371/journal.ppat.1002838.
24. **Karta MR, Gavala ML, Curran CS, Wickert LE, Keely PJ, Gern JE, Bertics PJ.** LPS modulates rhinovirus-induced chemokine secretion in monocytes and macrophages. *Am J Respir Cell Mol Biol* 51: 125–134, 2014. doi:10.1165/rcmb.2013-0404OC.
25. **Kenworthy AK.** Imaging protein-protein interactions using fluorescence resonance energy transfer microscopy. *Methods* 24: 289–296, 2001. doi:10.1006/meth.2001.1189.
26. **Kim EY, Battaile JT, Patel AC, You Y, Agapov E, Grayson MH, Benoit LA, Byers DE, Alevy Y, Tucker J, Swanson S, Tidwell R, Tyner JW, Morton JD, Castro M, Polineni D, Patterson GA, Schwendener RA, Allard JD, Peltz G, Holtzman MJ.** Persistent activation of an innate immune response translates respiratory viral infection into chronic lung disease. *Nat Med* 14: 633–640, 2008. doi:10.1038/nm1770.
27. **Kim HY, Chang YJ, Subramanian S, Lee HH, Albacker LA, Matangkasombut P, Savage PB, McKenzie AN, Smith DE, Rottman JB, DeKruyff RH, Umetsu DT.** Innate lymphoid cells responding to IL-33 mediate airway hyperreactivity independently of adaptive immunity. *J Allergy Clin Immunol* 129: 216–227.e6, 2012. doi:10.1016/j.jaci.2011.10.036.
28. **Korpi-Steiner NL, Bates ME, Lee WM, Hall DJ, Bertics PJ.** Human rhinovirus induces robust IP-10 release by monocytic cells, which is independent of viral replication but linked to type I interferon receptor ligation and STAT1 activation. *J Leukoc Biol* 80: 1364–1374, 2006. doi:10.1189/jlb.0606412.
29. **Lauener RP, Birchler T, Adamski J, Braun-Fahrländer C, Bufe A, Herz U, von Mutius E, Nowak D, Riedler J, Waser M, Sennhauser FH; ALEX study group.** Expression of CD14 and Toll-like receptor 2 in farmers' and non-farmers' children. *Lancet* 360: 465–466, 2002. doi:10.1016/S0140-6736(02)09641-1.
30. **Levental I, Lingwood D, Grzybek M, Coskun U, Simons K.** Palmitoylation regulates raft affinity for the majority of integral raft proteins. *Proc Natl Acad Sci USA* 107: 22050–22054, 2010. doi:10.1073/pnas.1016184107.
31. **Lewis JK, Bothner B, Smith TJ, Siuzdak G.** Antiviral agent blocks breathing of the common cold virus. *Proc Natl Acad Sci USA* 95: 6774–6778, 1998. doi:10.1073/pnas.95.12.6774.
32. **Manukyan M, Triantafilou K, Triantafilou M, Mackie A, Nilsen N, Espevik T, Wiesmüller KH, Ulmer AJ, Heine H.** Binding of lipopeptide to CD14 induces physical proximity of CD14, TLR2 and TLR1. *Eur J Immunol* 35: 911–921, 2005. doi:10.1002/eji.200425336.
33. **Martín-Belmonte F, López-Guerrero JA, Carrasco L, Alonso MA.** The amino-terminal nine amino acid sequence of poliovirus capsid VP4 protein is sufficient to confer N-myristoylation and targeting to detergent-insoluble membranes. *Biochemistry* 39: 1083–1090, 2000. doi:10.1021/bi992132e.
34. **Martorano LM, Grayson MH.** Respiratory viral infections and atopic development: from possible mechanisms to advances in treatment. *Eur J Immunol* 48: 407–414, 2018. doi:10.1002/eji.201747052.
35. **Meng G, Rutz M, Schiemann M, Metzger J, Grabiec A, Schwandner R, Luppa PB, Ebel F, Busch DH, Bauer S, Wagner H, Kirschning CJ.** Antagonistic antibody prevents toll-like receptor 2-driven lethal shock-like syndromes. *J Clin Invest* 113: 1473–1481, 2004. doi:10.1172/JCI20762.
36. **Morita H, Moro K, Koyasu S.** Innate lymphoid cells in allergic and nonallergic inflammation. *J Allergy Clin Immunol* 138: 1253–1264, 2016. doi:10.1016/j.jaci.2016.09.011.
37. **Mosser AG, Brockman-Schneider R, Amineva S, Burchell L, Sedgwick JB, Busse WW, Gern JE.** Similar frequency of rhinovirus-infectible cells in upper and lower airway epithelium. *J Infect Dis* 185: 734–743, 2002. doi:10.1086/339339.
38. **Nagarkar DR, Bowman ER, Schneider D, Wang Q, Shim J, Zhao Y, Linn MJ, McHenry CL, Gosangi B, Bentley JK, Tsai WC, Sajjan US, Lukacs NW, Hershenson MB.** Rhinovirus infection of allergen-sensitized and -challenged mice induces eotaxin release from functionally polarized macrophages. *J Immunol* 185: 2525–2535, 2010. doi:10.4049/jimmunol.1000286.
39. **Nagarkar DR, Wang Q, Shim J, Zhao Y, Tsai WC, Lukacs NW, Sajjan U, Hershenson MB.** CXCR2 is required for neutrophilic airway inflammation and hyperresponsiveness in a mouse model of human rhinovirus infection. *J Immunol* 183: 6698–6707, 2009. doi:10.4049/jimmunol.0900298.
40. **Newcomb DC, Sajjan U, Nanua S, Jia Y, Goldsmith AM, Bentley JK, Hershenson MB.** Phosphatidylinositol 3-kinase is required for rhinovirus-induced airway epithelial cell interleukin-8 expression. *J Biol Chem* 280: 36952–36961, 2005. doi:10.1074/jbc.M502449200.
41. **Newcomb DC, Sajjan US, Nagarkar DR, Wang Q, Nanua S, Zhou Y, McHenry CL, Hennrick KT, Tsai WC, Bentley JK, Lukacs NW, Johnston SL, Hershenson MB.** Human rhinovirus 1B exposure induces phosphatidylinositol 3-kinase-dependent airway inflammation in mice. *Am J Respir Crit Care Med* 177: 1111–1121, 2008. doi:10.1164/rccm.200708-1243OC.
42. **Nilsen NJ, Vladimer GI, Stenvik J, Orning MPA, Zeid-Kilani MV, Bugge M, Bergstroem B, Conlon J, Husebye H, Hise AG, Fitzgerald KA, Espevik T, Lien E.** A role for the adaptor proteins TRAM and TRIF in toll-like receptor 2 signaling. *J Biol Chem* 290: 3209–3222, 2015. doi:10.1074/jbc.M114.593426.
43. **Panjwani A, Strauss M, Gold S, Wenham H, Jackson T, Chou JJ, Rowlands DJ, Stonehouse NJ, Hogle JM, Tuthill TJ.** Capsid protein VP4 of human rhinovirus induces membrane permeability by the formation of a size-selective multimeric pore. *PLoS Pathog* 10: e1004294, 2014. doi:10.1371/journal.ppat.1004294.
44. **Pauligk C, Nain M, Reiling N, Gemsa D, Kaufmann A.** CD14 is required for influenza A virus-induced cytokine and chemokine production. *Immunobiology* 209: 3–10, 2004. doi:10.1016/j.imbio.2004.04.002.
45. **Roszik J, Szöllosi J, Vereb G.** AccPbFRET: an ImageJ plugin for semi-automatic, fully corrected analysis of acceptor photobleaching FRET images. *BMC Bioinformatics* 9: 346, 2008. doi:10.1186/1471-2105-9-346.
46. **Roy R, Hohng S, Ha T.** A practical guide to single-molecule FRET. *Nat Methods* 5: 507–516, 2008. doi:10.1038/nmeth.1208.
47. **Saba TG, Chung Y, Hong JY, Sajjan US, Bentley JK, Hershenson MB.** Rhinovirus-induced macrophage cytokine expression does not require endocytosis or replication. *Am J Respir Cell Mol Biol* 50: 974–984, 2014. doi:10.1165/rcmb.2013-0354OC.
48. **Schneider D, Ganesan S, Comstock AT, Meldrum CA, Mahidhara R, Goldsmith AM, Curtis JL, Martinez FJ, Hershenson MB, Sajjan U.**

Increased cytokine response of rhinovirus-infected airway epithelial cells in chronic obstructive pulmonary disease. *Am J Respir Crit Care Med* 182: 332–340, 2010. doi:10.1164/rccm.200911-1673OC.

49. **Schneider D, Hong JY, Bowman ER, Chung Y, Nagarkar DR, McHenry CL, Goldsmith AM, Bentley JK, Lewis TC, Hershenson MB.** Macrophage/epithelial cell CCL2 contributes to rhinovirus-induced hyperresponsiveness and inflammation in a mouse model of allergic airways disease. *Am J Physiol Lung Cell Mol Physiol* 304: L162–L169, 2013. doi:10.1152/ajplung.00182.2012.
50. **Soong G, Reddy B, Sokol S, Adamo R, Prince A.** TLR2 is mobilized into an apical lipid raft receptor complex to signal infection in airway epithelial cells. *J Clin Invest* 113: 1482–1489, 2004. doi:10.1172/JCI200420773.
51. **Stack J, Doyle SL, Connolly DJ, Reinert LS, O'Keeffe KM, McLoughlin RM, Paludan SR, Bowie AG.** TRAM is required for TLR2 endosomal signaling to type I IFN induction. *J Immunol* 193: 6090–6102, 2014. doi:10.4049/jimmunol.1401605.
52. **Suzuki T, Yamaya M, Sekizawa K, Hosoda M, Yamada N, Ishizuka S, Nakayama K, Yanai M, Numazaki Y, Sasaki H.** Bafilomycin A_1 inhibits rhinovirus infection in human airway epithelium: effects on endosome and ICAM-1. *Am J Physiol Lung Cell Mol Physiol* 280: L1115–L1127, 2001. doi:10.1152/ajplung.2001.280.6.L1115.
53. **Triantafilou K, Vakakis E, Richer EA, Evans GL, Villiers JP, Triantafilou M.** Human rhinovirus recognition in non-immune cells is mediated by Toll-like receptors and MDA-5, which trigger a synergetic pro-inflammatory immune response. *Virulence* 2: 22–29, 2011. doi:10.4161/viru.2.1.13807.
54. **Triantafilou M, Gamper FG, Haston RM, Mouratis MA, Morath S, Hartung T, Triantafilou K.** Membrane sorting of toll-like receptor (TLR)-2/6 and TLR2/1 heterodimers at the cell surface determines heterotypic associations with CD36 and intracellular targeting. *J Biol Chem* 281: 31002–31011, 2006. doi:10.1074/jbc.M602794200.
55. **Triantafilou M, Lepper PM, Olden R, Dias IS, Triantafilou K.** Location, location, location: is membrane partitioning everything when it comes to innate immune activation? *Mediators Inflamm* 2011: 186093, 2011. doi:10.1155/2011/186093.
56. **Triantafilou M, Manukyan M, Mackie A, Morath S, Hartung T, Heine H, Triantafilou K.** Lipoteichoic acid and toll-like receptor 2 internalization and targeting to the Golgi are lipid raft-dependent. *J Biol Chem* 279: 40882–40889, 2004. doi:10.1074/jbc.M400466200.
57. **van Bergenhenegouwen J, Plantinga TS, Joosten LAB, Netea MG, Folkerts G, Kraneveld AD, Garssen J, Vos AP.** TLR2 & Co: a critical analysis of the complex interactions between TLR2 and coreceptors. *J Leukoc Biol* 94: 885–902, 2013. doi:10.1189/jlb.0113003.
58. **Vasselon T, Detmers PA, Charron D, Haziot A.** TLR2 recognizes a bacterial lipopeptide through direct binding. *J Immunol* 173: 7401–7405, 2004. doi:10.4049/jimmunol.173.12.7401.
59. **Verveer PJ, Rocks O, Harpur AG, Bastiaens PI.** Imaging protein interactions by FRET microscopy: cell preparation for FRET analysis. *CSH Protoc* 2006: pdb.prot4646, 2006. doi:10.1101/pdb.prot4646.
60. **Wang Q, Miller DJ, Bowman ER, Nagarkar DR, Schneider D, Zhao Y, Linn MJ, Goldsmith AM, Bentley JK, Sajjan US, Hershenson MB.** MDA5 and TLR3 initiate pro-inflammatory signaling pathways leading to rhinovirus-induced airways inflammation and hyperresponsiveness. *PLoS Pathog* 7: e1002070, 2011. doi:10.1371/journal.ppat.1002070.
61. **Wang Q, Nagarkar DR, Bowman ER, Schneider D, Gosangi B, Lei J, Zhao Y, McHenry CL, Burgens RV, Miller DJ, Sajjan U, Hershenson MB.** Role of double-stranded RNA pattern recognition receptors in rhinovirus-induced airway epithelial cell responses. *J Immunol* 183: 6989–6997, 2009. doi:10.4049/jimmunol.0901386.
62. **Weischenfeldt J, Porse B.** Bone marrow-derived macrophages (BMM): isolation and applications. *CSH Protoc* 2008: pdb.prot5080, 2008. doi:10.1101/pdb.prot5080.
63. **Wickert LE, Karta MR, Audhya A, Gern JE, Bertics PJ.** Simvastatin attenuates rhinovirus-induced interferon and CXCL10 secretion from monocytic cells in vitro. *J Leukoc Biol* 95: 951–959, 2014. doi:10.1189/jlb.0713413.